HgCdTe superlattices for solid-state cryogenic refrigeration

D Vashaee A Shakouri

HgCdTe superlattices for solid-state cryogenic refrigeration

Abstract

A tall barrier superlattice structure based on mercury cadmium telluride material system is proposed that can achieve a large effective thermoelectric figure of merit (ZT(max)similar to 3) at cryogenic temperatures. Calculations based on the Boltzmann transport equation taking into account the quantum mechanical electron transmission show that the Seebeck coefficient can be increased significantly at low temperatures with the use of nonplanar barriers as the thermal spreading of the electron density is tightened around the Fermi level. This provides a better asymmetric differential conductivity around the Fermi level close to the top of the barrier. Consequently, a high thermoelectric power factor is produced resulting in a large ZT. (c) 2006 American Institute of Physics.

HgCdTe superlattices for solid-state cryogenic refrigeration

Daryoosh Vashaee[a] and Ali Shakouri
Jack Baskin School of Engineering, University of California, Santa Cruz, California 95064

(Received 24 August 2005; accepted 7 March 2006; published online 29 March 2006)

A tall barrier superlattice structure based on mercury cadmium telluride material system is proposed that can achieve a large effective thermoelectric figure of merit ($ZT_{max} \sim 3$) at cryogenic temperatures. Calculations based on the Boltzmann transport equation taking into account the quantum mechanical electron transmission show that the Seebeck coefficient can be increased significantly at low temperatures with the use of nonplanar barriers as the thermal spreading of the electron density is tightened around the Fermi level. This provides a better asymmetric differential conductivity around the Fermi level close to the top of the barrier. Consequently, a high thermoelectric power factor is produced resulting in a large *ZT*. © *2006 American Institute of Physics*. [DOI: 10.1063/1.2191094]

Although there are several thermoelectric materials that work well at high temperature,[1–6] for cryogenic refrigeration the situation is entirely different. To date there are only two suitable materials for low temperature applications: bismuth-antimony telluride[7] (BiSbTe) and bismuth-antimony (Bi–Sb) alloys.[8] Nevertheless, the material properties are too poor to build an entire solid-state refrigerator capable of cooling the range from room temperature down to liquid nitrogen (77 K) where some high temperature superconductors could operate.[9] These material systems achieve a *ZT* of about 0.6 over a wide temperature range. However, there is an increasing need for materials with a *ZT* of 1 or more at low temperatures.[10] Such new materials could make many superconducting devices practical.

Heterostructure integrated thermionic microrefrigerator[11–14] has been proposed for room-temperature application. High figure of merit *ZT* has been predicted for metallic superlattices at 300 K.[15] In this letter, we will extend the previous work to low temperatures and propose to use novel mercury cadmium telluride (MCT) superlattices for these applications.[16] There have been previous studies of thermoelectric refrigeration in HgCdTe superlattices.[17] However, only compositions with small barrier height were considered and conserved transverse momentum was assumed.[18] We will show that tall barrier MCT system has potential to achieve $ZT \sim 3$ at 100 K.

$Hg_xCd_{1-x}Te$ material is studied extensively because of its use as infrared detectors. Most of the parameters needed for transport calculations are available in the literature, such as the energy gap $E_g(x)$, electron and hole effective masses, thermal conductivity, etc.[19–22] However, since there have been few applications where highly degenerated MCT alloys were desired, there are not enough data to quantify the carrier mobility at doping levels of $N_D > 10^{18}-10^{19}$ cm^{-3}, where thermionic coolers exhibit their superior performance. In what follows, we attempt to make some reasonable assumptions about the mobility at high doping densities and extrapolate the available experimental data to higher doping levels.[23] Electron mobility affects the material figure of merit and, as seen in Fig. 1, it strongly depends on the doping concentration.

Alloying the $Hg_xCd_{1-x}Te$ system permits a wide range of energy gap values. For thermoelectrics, adamantine materials generally have a high value of thermal conductivity.[24] Alloying reduces their thermal conductivity. However, a MCT alloy does not have a high *ZT* value. The thermoelectric properties of MCT for bulk materials and superlattices have already been studied, see Ref. 16. However, we will revisit this study since an important consideration, mobility variations with doping concentration, was not addressed there. Figure 2 shows the calculated electrical conductivity (σ), Seebeck coefficient (S), Fermi energy (E_F), and thermoelectric figure of merit (ZT) versus doping concentration of $Hg_{0.8}Cd_{0.2}Te$ bulk materials at two temperatures, 100 and 300 K. We see that the value of *ZT* at $T=100$ K is very small ($ZT \sim 0.01$). This is true for any value of the alloy fraction x or at any value of the energy gap.[10] We conclude that $Hg_{1-x}Cd_xTe$ bulk is not a good TE material, particularly at low temperatures. At $T=300$ K the maximum attainable *ZT* is about one-third (this is for $x=0.2$). This value is too low to be useful in thermoelectric devices. The main reason for the low *ZT* value is that $Hg_xCd_{1-x}Te$ has one conduction band. Good thermoelectric materials such as Bi_2Te_3 based semiconductors[19] have numerous valleys. It is possible to have a large *ZT* with a single conduction band if the material has higher effective mass. This will increase the density of states near the conduction band minimum. However, as thermionic emissions in heterostructures relax the need for a

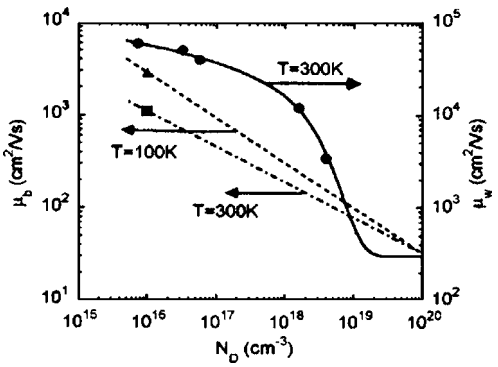

FIG. 1. Electron mobility in the well (solid) and barrier (dash and dash-dot) regions vs doping concentration. Symbols show the experimental data and curves show the corresponding fitting (Ref. 23).

[a]Electronic mail: daryoosh@soe.ucsc.edu

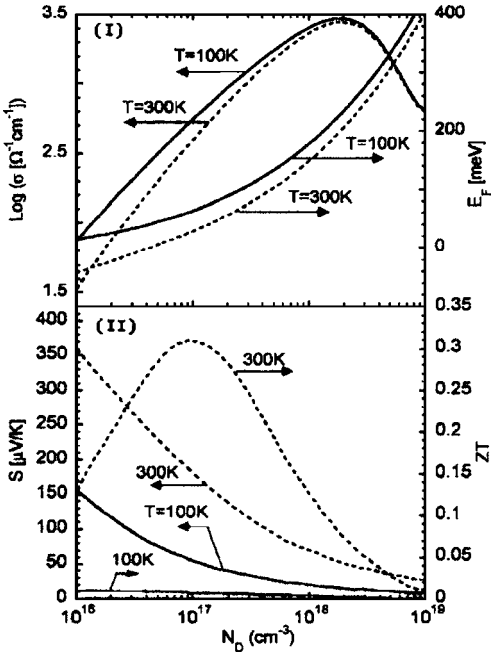

FIG. 2. Electrical conductivity [(I) left axis], Fermi energy [(I) right axis], Seebeck coefficient [(II) left axis], and thermoelectric figure of merit [(II) right axis] of $Hg_{0.8}Cd_{0.2}Te$ bulk at $T=300$ K (solid) and $T=100$ K (dashed).

large effective mass (m^*), the capability of having a large potential barrier height in a MCT superlattice system makes it a good candidate for heterostructure thermionic refrigeration.

For the calculation of the transport coefficient of MCT, we use the model presented in Ref. 16. In brief, a linear Boltzmann transport equation was used to calculate the thermoelectric characteristics of the MCT bulk device. As for the superlattice properties, a conventional bulk transport was modified, taking into account the two-dimensional (2D) states in the well and three-dimensional (3D) states above the well and in the barrier. In addition, the quantum mechanical transmission coefficient for electron transport between wells was introduced in the Boltzmann equation. This takes into account both tunneling and thermionic emission. Since the barrier layer thickness is large enough for miniband transport to be negligible, transmission probability is calculated using the Wentzel-Kramer-Brillouin (WKB) approximation. Finally, Fermi-Dirac statistics was used to account for the number of available empty states in the neighboring wells for tunneling and thermionic emission calculations.

We will hereby present the results from the calculations of the thermoelectric properties of the MCT superlattice. Parameters used in the simulations are listed in Table I, where n_w is the number of superlattice periods, L_w and L_b are the widths of well and barrier, respectively, V_b is the barrier height, m_e^* is the electron's effective mass, β is the thermal conductivity, and α is the nonparabolicity of the conduction band. There are eight energy levels calculated in the well: 67.4, 166.2, 267.7, 369.7, 471.4, 572.3, 671.6, and 767.3 meV at 100 K and 51.8, 143.9, 243.1, 343.9, 444.9, 544.8, 641.8, and 727.3 meV at 300 K.

To check the thermoelectric properties of the MCT superlattice versus doping concentration, there are three cases to be considered: only the well region is doped and the barrier is undoped, only the barrier is doped, or both regions are uniformly doped. The mobility of each layer could be different in the above three cases due to impurity scattering. Since the superlattice period is smaller than the electron mean free path, the effective mobility is expected to be an average of the well and barrier regions' mobility values. One may benefit by putting all dopings in the barrier. This modulation doping gives a charge in the $Hg_{0.8}Cd_{0.2}Te$ wells without the reduced mobility that results from ionized donor scattering. This can result in a higher average electron mobility in the cross-plane transport as well. In the case where all doping occurs in the well region, it turns out that ZT is significantly reduced, as the optimum value of ZT happens at a very large doping concentration. On the other hand, the situation seems to be different when the barrier is doped and the well is undoped. Electron mobility in the barrier region is already small due to the large value of x, and it is further reduced with the increased doping concentration. Nevertheless, the electron mobility in the well region remains significantly high when it is undoped (in the order of 1 $m^2/V\,s$ at $T=300$ K and 9 $m^2/V\,s$ at $T=100$ K). In fact, the average mobility is much larger when the well region is not doped.

For comparison with the bulk values of Fig. 2, the same parameters are calculated at room temperature while assuming that all doping is in the barrier region. In calculations, two cases are considered: when transverse momentum during thermionic emission is conserved and when transverse momentum is not conserved. Detailed theoretical calculations[28–30] and experimental results[31] have shown that nonplanar interfaces give rise to significant current increase due to nonconservation of transverse momentum. In brief, interaction of the quantized charge carriers in the quantum well with inhomogeneities or nonplanar barrier can couple the in-plane and perpendicular to the plane degrees of freedom and break the conservation of transverse momentum. This significantly increases the number of electrons that are transmitted over the barrier. These electrons are responsible for thermionic cooling, and thereby thermionic cooling power is increased.[15,16]

A significant improvement in ZT is predicted in Fig. 3(II) (dashed lines). A maximum ZT of about 2.3 is predicted at about 1.7×10^{19} cm^{-3} when the transverse momentum is not conserved. To emphasize that the cooling improvement is solely due to the thermionic emission of electrons over the barrier, we are not considering reduction in lattice thermal conductivity in our comparison of bulk and superlattice

TABLE I. Parameters used in the simulations of $Hg_{1-x}Cd_xTe$ superlattice.

Well/barrier	n_w	L_w (nm)	L_b (nm)	V_b (meV)[a] (300 K/100 K)	m_e^*/m_e (well/barrier)	β (W/mK)[b] (300 K/100 K)	α (eV^{-1})[c] (well/barrier)
$Hg_{0.8}Cd_{0.2}Te/Hg_{0.2}Cd_{0.8}Te$	20	20	40	731/835	0.01/0.07	0.97/2	6.3/0.8

[a]Reference 25.
[b]Reference 26.
[c]Reference 27.

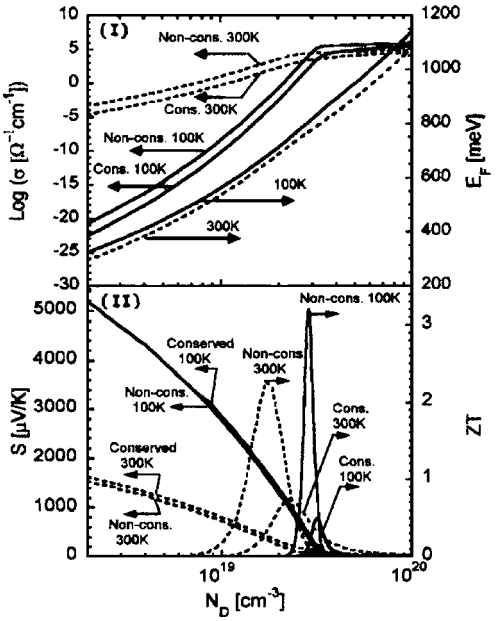

FIG. 3. Electrical conductivity [(I) left axis], Fermi energy [(I) right axis], Seebeck coefficient [(II) left axis], and thermoelectric figure of merit [(II) right axis] of $Hg_{0.8}Cd_{0.2}Te/Hg_{0.2}Cd_{0.8}Te$ superlattice for two cases of conserved and nonconserved transverse momentum at 100 K (solid) and 300 K (dashed).

structures. Considering it will cause an even higher *ZT* in HgCdTe superlattices. *ZT* is inversely proportional to thermal conductivity. Figure 3 shows the calculated thermoelectric properties of the $Hg_{0.2}Cd_{0.8}Te/Hg_{0.8}Cd_{0.2}Te$ superlattice at $T=100$ K (solid lines). It is assumed again that all doping is in the barrier. A significant improvement in *ZT* is predicted. An optimum *ZT* of about 3.2 is predicted when the transverse momentum is not conserved.

We already predicted a *ZT* of about 2 at room temperature for a similar superlattice at slightly different doping values. However, at a low temperature ($T=100$ K) we predict a *ZT* of 0.5 in the case where transverse momentum is conserved and a *ZT* of 3.2 in the case where the transverse momentum is not conserved. This is very promising considering the highest *ZT* measured at low temperatures, specifically 225 K, has been only 0.8. This value was achieved for bulk $CsBi_4Te_6$ material.[32] Moreover, there is no new thermoelectric material that works below 200 K.

In summary, improved thermoelectric properties in heterostructure's thermionic emission coolers at low temperatures were explored. Mercury cadmium telluride (MCT) superlattices are proposed for low temperature cooling applications. Since CdTe and HgTe have virtually the same lattice constants, the $Hg_xCd_{1-x}Te$ system permits a wide range of energy gaps by alloying. Tall barrier MCT superlattices, when doped appropriately, exhibit more than two orders of magnitude improvement in *ZT* ($ZT\sim3$ at 100 K). The main reason for the low value of *ZT* in MCT bulk is that it has a very low effective mass and a single conduction band. Thermionic emissions in heterostructures loosen up the high effective mass requirement since the improvement in the Seebeck coefficient is achieved via the induced asymmetric differential conductivity by a potential barrier. At a low temperature, the thermal spreading of the electron density is narrower around the Fermi level. Thus, the potential barrier generates a larger asymmetric differential conductivity around the Fermi level close to the top of the barrier, which results in a higher Seebeck coefficient. The optimum thermoelectric figure of merit is improved accordingly. This improvement can be combined with other techniques to reduce lattice thermal conductivity and achieve higher *ZT* values.

This work was supported by ONR MURI Thermionic Energy Conversion Center.

[1]F. D. Rosi, J. P. Dismukes, and E. F. Hockings, Electr. Eng. **79**, 450 (1960).
[2]C. Wood, Rep. Prog. Phys. **51**, 459 (1988).
[3]B. Abeles, D. S. Beers, G. D. Cody, and J. P. Dismukes, Phys. Rev. **125**, 340 (1962).
[4]C. B. Vining, J. Appl. Phys. **69**, 331 (1991).
[5]B. C. Sales, D. Mandrus, and R. K. Williams, Science **272**, 1325 (1996).
[6]J. P. Fleurial, A. Borshchevsky, T. Caillat, D. T. Morelli, and G. P. Meisner, International Conference on Thermoelectrics (ICT, 1996), pp. 91–95.
[7]C. H. Champness, P. T. Chiang, and P. Parekh, Can. J. Phys. **43**, 653 (1965).
[8]W. M. Yim and A. Smith, Solid-State Electron. **15**, 1141 (1972).
[9]For a review, see M. G. Kanatzidis, Semicond. Semimetals **69**, 51 (2001).
[10]G. D. Mahan, *Solid State Physics* (Academic, New York, 1998), Vol. 51.
[11]A. Shakouri and J. E. Bowers, Appl. Phys. Lett. **71**, 1234 (1997).
[12]A. Shakouri, E. Y. Lee, D. L. Smith, V. Narayanamurti, and J. E. Bowers, Microscale Thermophys. Eng. **2**, 37 (1998).
[13]X. F. Fan, G. Zeng, E. Croke, C. LaBounty, C. C. Ahn, D. Vashaee, A. Shakouri, and J. E. Bowers, Electron. Lett. **37**, 126 (2001).
[14]C. LaBounty, A. Shakouri, and J. E. Bowers, J. Appl. Phys. **89**, 4059 (2001).
[15]D. Vashaee and A. Shakouri, Phys. Rev. Lett. **92**, 106103 (2004).
[16]D. Vashaee and A. Shakouri, J. Appl. Phys. **95**, 1233 (2004).
[17]R. J. Radtke, H. Ehrenreich, and C. H. Grein, J. Appl. Phys. **86**, 3195 (1999).
[18]See Ref. 16 for more detailed comparison of the present structure with that of Ref. 17.
[19]T. C. Harman, A. J. Strauss, D. H. Hickey, M. S. Dresselhaus, G. B. Wright, and J. G. Mavroides, Phys. Rev. Lett. **7**, 403 (1961).
[20]*Semiconductors and Semimetals*, edited by R. K. Willardson and A. C. Beer (Academic, New York, 1981), Vol. 16.
[21]C. Fau, J. F. Dame, M. de Carvalho, J. Calas, M. Averous, and B. A. Lombos, Phys. Status Solidi B **125**, 831 (1984).
[22]R. Grill, Phys. Rev. B **46**, 2092 (1992).
[23]For $x=0.2$ and $T=300$ K mobility values are taken from R. G. Benz II, A. Conte-Matos, B. K. Wagner, and C. J. Summers, Appl. Phys. Lett. **65**, 2836 (1994), assuming $\mu(x=0.2)\sim\mu(x=0.24)$. High doping concentration mobility is estimated to saturate to ~300 cm^2/V s. At $T=100$ K and low doping concentration, mobility is about 9 m^2/V s. At $T=100$ K and high doping concentrations, it is assumed that $\mu(T=100\text{ K})\sim\mu(T=300\text{ K})$. For $x=0.8$ and high doping concentration, where the optimum *ZT* happens, it is assumed that $\mu(T=100\text{ K})\sim\mu(T=300\text{ K})$.
[24]G. A. Slack, in *Solid State Physics*, edited by H. Ehrenreich, F. Seitz, and D. Turnbull (Academic, New York, 1979), Vol. 34.
[25]Energy band parameters are extracted from Landolt-Bornstein online library; see J. Chu, S. Xu, and D. Tang, Appl. Phys. Lett. **43**, 1064 (1983).
[26]J. O. Sofo, G. D. Mahan, and J. Baars, J. Appl. Phys. **76**, 2249 (1994) [they have used tabulated values by J. C. Brice, in *Properties of Mercury Cadmium Telluride*, EMIS Data Reviews Ser. No. 3, edited by J. Brice and P. Capper (The Institution of Electrical Engineers, Surrey, England, 1987), p. 16].
[27]Nonparabolicity of the conduction band is approximated using $\alpha\sim1/E_g(1-m_e^*)^2$.
[28]D. L. Smith, E. Y. Lee, and V. Narayanamurti, Phys. Rev. Lett. **80**, 2433 (1998).
[29]Daryoosh Vashaee and Ali Shakouri, Mater. Res. Soc. Symp. Proc. **691**, 131 (2001).
[30]D. L. Smith, M. Kozhevnikov, E. Y. Lee, and V. Narayanamurti, Phys. Rev. B **61**, 13914 (2000).
[31]M. Kozhevnikov, V. Narayanamurti, C. Zheng, Yi-Jen Chiu, and D. L. Smith, Phys. Rev. Lett. **82**, 3677 (1999).
[32]Duck-Young Chung, Tim Hogan, Paul Brazis, Melissa Rocci-Lane, Carl Kannewurf, Marina Bastea, Ctirad Uher, and Mercouri G. Kanatzidis, Science **287**, 1024 (2000).